$(CuI)_3P_4S_4$: Preparation, Structural, and NMR Spectroscopic Characterization of a Copper(I) Halide Adduct with β-P_4S_4

Sara Reiser,[a] Gunther Brunklaus,[b] Jung Hoon Hong,[a] Jerry C. C. Chan,[b]+ Hellmut Eckert,*[b] and Arno Pfitzner*[a]

Abstract: $(CuI)_3P_4S_4$ is obtained by reaction of stoichiometric amounts of CuI, P, and S in evacuated silica ampoules. The yellow compound consists of monomeric β-P_4S_4 cage molecules that are separated by hexagonal columns of CuI. $(CuI)_3P_4S_4$ crystallizes isotypic to $(CuI)_3P_4Se_4$ in the hexagonal system, space group $P6_3cm$ (no. 185) with $a = 19.082(3)$, $c = 6.691(1)$ Å, $V = 2109.9(6)$ Å^3, and $Z = 6$. Three of the four phosphorus atoms are bonded to copper, whereas no bonds between copper and sulfur are observed. The two crystallographically distinct copper sites are clearly differentiated by ^{65}Cu magic-angle spinning (MAS) NMR spectroscopy. Furthermore, an unequivocal assignment of the ^{31}P MAS-NMR spectra is possible on the basis of homo- and heteronuclear dipole–dipole and scalar interactions. Dipolar coupling to the adjacent quadrupolar spins ^{63,65}Cu generates a clear multiplet structure of the peaks attributable to P1 and P2, respectively. Furthermore, the utility of a newly developed two-dimensional NMR technique is illustrated to reveal direct connectivity between P atoms based on (^{31}P–^{31}P) scalar interactions.

Keywords: cage compounds · copper · dipole–dipole interactions · NMR spectroscopy · phosphorus · sulfur

Introduction

The use of copper(I) halides as a preparative tool for the synthesis of neutral or low-charged phosphorus polymers and phosphorus–selenide cage molecules has recently been established.[1] Thus, the hitherto unknown phosphorus–selenide molecules P_8Se_3 and β-P_4Se_4 could be obtained as their copper iodide adducts $(CuI)_2P_8Se_3$ and $(CuI)_3P_4Se_4$, respectively.[2, 3] Chiral polymeric P_4Se_4 tubes observed in *catena*-$(P_4Se_4)_x$[4] are transferred to achiral polymers of the same composition upon embedding them in copper iodide.[5] Evidently, the reactivity of mixtures of elemental phosphorus and selenium remains unchanged when the reactions are performed in copper iodide. However, the uncontrolled formation of polymeric structures upon lowering the reaction temperature is suppressed by embedding the reaction products in copper iodide. The formation of adduct compounds with phosphorus chalcogenide molecules is not restricted to Cu^+. An example of a closely related adduct of the β-P_4S_4 cage to another transition metal is $[\beta$-$P_4S_4(NbCl_5)_2]$.[6] We recently started to elucidate the utility of CuI as a reaction medium also for the formation of phosphorus sulfide cages. Previous attempts to prepare ligand-free α-P_4S_4 and β-P_4S_4 from the elements at low temperatures ($T < 100\,^\circ$C) led to a mixture of different phosphorus sulfides, containing the above-mentioned compounds only as minor reaction products.[7] Polycrystalline β-P_4S_4 has also been obtained by the reaction of P_4S_5 and $P(C_6H_5)_3$ in cold CS_2,[8] and its molecular structure has been derived from ^{31}P NMR spectroscopic data only.[9]

Herein we report the preparation and structural characterization of $(CuI)_3P_4S_4$. The molecular structure of the β-P_4S_4 cages therein is compared to those in $[\beta$-$P_4S_4(NbCl_5)_2]$. In addition we present a comprehensive solid-state NMR characterization of this compound, based on state-of-the-art high-resolution techniques. In this context the recovery of homo- and heteronuclear dipole–dipole and scalar interactions is of particular significance for unequivocal peak assignments and for gaining valuable structural information.

[a] Prof. Dr. A. Pfitzner, S. Reiser, J. H. Hong
Universität Regensburg, Institut für Anorganische Chemie
93040 Regensburg (Germany)
Fax: (+49) 941 943 4983
E-mail: arno.pfitzner@chemie.uni-regensburg.de

[b] Prof. Dr. H. Eckert, G. Brunklaus, J. C. C. Chan+
Westfälische Wilhelms-Universität Münster
Institut für Physikalische Chemie
48149 Münster (Germany)
Fax: (+49) 251 83 29159
E-mail: eckerth@uni-muenster.de

[+] Present address: Laboratory of Chemical Physics, National Institute of Health, Bethesda, MD 20892 (USA)

Results and Discussion

Crystal structure: The crystal structure of $(CuI)_3P_4S_4$ was determined by X-ray diffraction from a single crystal at room

0947-6539/02/0818-4228 $ 20.00+.50/0

Table 1. Crystallographic data of $(CuI)_3P_4S_4$.[a]

compound	$(CuI)_3P_4S_4$
M_r [g mol^{-1}]	823.44
crystal size [mm^3]	0.24 × 0.025 × 0.02
crystal system	hexagonal
space group	$P6_3cm$
a [Å]	19.082(3)
c [Å]	6.691(1)
V [Å^3], Z	2109.9(6), 6
$\rho_{calculated}$ [g cm^{-1}]	3.888
$\mu(Mo_{K\alpha})$ [mm^{-1}]	12.085
diffractometer	STOE IPDS, $Mo_{K\alpha}$, $\lambda = 0.71073$ Å
image plate distance [mm]	60.0
ϕ-range [°], $\Delta\phi$ [°]	$-2 \le \phi \le 186$, 1.0
no. of frames	188
exposure time/frame [min]	9.00
$2\theta_{max}$ [°]	56.34
hkl range	$-25 \le h \le 25$ $-25 \le k \le 25$ $-8 \le l \le 8$
no. of reflections	19430
no. of independent reflections, $R_{int.}$	1771, 0.1172
no. of reflections with $I > 2\sigma(I)$	1451
number of parameters	74
refinement program	SHELX-97[10]
R ($I > 2\sigma(I)$), R (all reflections)	0.0316, 0.0403
wR ($I > 2\sigma(I)$), wR (all reflections)[b]	0.0701, 0.0735
GooF	1.007
inversion twin part	0.18
largest difference peaks $\Delta\rho_{min}$, $\Delta\rho_{max}$ [e Å^{-3}]	−0.95, 1.72

[a] Further details of the crystal structure investigation can be obtained from the Fachinformationszentrum Karlsruhe, 76344 Eggenstein-Leopoldshafen, Germany (fax: (+49)7247-808-666; e-mail: crysdata@fiz-karlsruhe.de) on quoting the depository number CSD-412533. [b] $w = 1/[\sigma^2(F_o^2) + (0.0387\,P)^2]$, $P = [\max(F_o^2, 0) + 2F_c^2]/3$.

temperature. A total of 74 parameters including anisotropic displacement parameters and an inversion twin option were used to refine (SHELXL97[10]) the model to the final R values $R = 0.0316$ and $wR = 0.0701$ ($I > 2\sigma$) (see Table 1 for details). $(CuI)_3P_4S_4$ crystallizes isotypic to the hexagonal compound $(CuI)_3P_4Se_4$. However, a small difference concerning the distribution of the copper atoms has to be mentioned (vide infra). Atomic positions are given in Table 2, selected interatomic distances in Table 3.

$(CuI)_3P_4S_4$ consists of β-P_4S_4 cages (Figure 1 a) which are stacked along [001]. These cage molecules with C_s symmetry may be derived from the well known P_4S_3 cage by insertion of an additional sulfur atom into the basal P_3 ring. The shortest intermolecular distances between the cages are about $d(S1{-}S3) = 3.3$ Å. Three of the four phosphorus atoms (P1, P2, P2′) but none of the sulfur atoms are coordinated to the copper center (see Table 3 for distances). Both copper atoms are located in a distorted tetrahedral environment surrounded by one phosphorus and three iodine atoms. These tetrahedra separate the β-P_4S_4 cages, both along the stacks and perpendicular to the stacks ($d(S{-}S) > 4$ Å, see Figure 1 b). The tetrahedra are arranged to form columns along the c axis. From Figure 2 it becomes evident that there exist two crystallographically different types of such columns, one of them with the top of the tetrahedra towards the viewer and the other one oriented the opposite way. Both columns have their building principle in common. Thus, they can be described as sections from the wurtzite structure type, which is not yet known for pure copper iodide. The mutual orientation of the columns has already been discussed in detail.[3] However, the copper positions are fully occupied in the crystal structure of $(CuI)_3P_4S_4$, whereas a certain disorder of copper is observed in the homologous compound $(CuI)_3P_4Se_4$. The better fit of β-P_4S_4 and the copper iodide matrix as compared to β-P_4Se_4 might be an explanation for this finding.

A comparison of the β-P_4S_4 cages stabilized by CuI and by $NbCl_5$,[6] respectively, reveals only slight differences with respect to bond lengths and angles within the cage molecules. The β-P_4S_4 cage in $[\beta\text{-}P_4S_4(NbCl_5)_2]$ is coordinated only to two Nb atoms through P2 and P2′. By contrast, an additional metal

Table 2. Atomic coordinates and displacement parameters U_{eq}[a] (in Å^2) for $(CuI)_3P_4S_4$ at 298 K.

Atom	Wyckoff positions	x	y	z	U_{eq}
I1	6c	0.13279(3)	x	0.7071(1)	0.0205(2)
I2	12d	0.19860(3)	0.53194(3)	0.08692(8)	0.0225(1)
Cu1	6c	0.12585(7)	x	0.3159(3)	0.0237(3)
Cu2	12d	0.33320(5)	0.53916(6)	−0.0155(2)	0.0281(3)
P1	6c	0.2372(1)	x	0.2182(5)	0.0202(5)
P2	12d	0.33631(9)	0.4276(1)	0.0725(4)	0.0214(4)
P3	6c	0.4008(1)	x	0.3173(4)	0.0222(6)
S1	6c	0.3052(1)	x	0.4649(4)	0.0253(5)
S2	12d	0.22096(9)	0.3240(1)	0.0640(4)	0.0260(4)
S3	6c	0.4106(2)	x	-0.1338(5)	0.0270(6)

[a] U_{eq} is defined as one third of the trace of the orthogonalized U^{ij} tensor.

Table 3. Selected interatomic distances [Å] and angles [°] for $(CuI)_3P_4S_4$.

Cu1–I1 2×	2.5755(9)	P1–S1	2.099(4)
Cu1–I1	2.621(2)	P1–S2 2×	2.102(3)
Cu1–P1	2.224(3)	P2–S2	2.098(2)
Cu2–I2	2.595(1)	P2–S3	2.116(3)
Cu2–I2	2.598(1)	P2–P3	2.256(3)
Cu2–I2	2.664(2)	P3–S1	2.075(4)
Cu2–P2	2.238(2)	P3–P2 2×	2.256(3)
S1-P1-S2 2×	100.9(1)	S1-P3-P2 2×	101.9(1)
S2-P1-S2	108.3(2)	P2-P3-P2	83.9(2)
S2-P2-S3	107.8(1)	P1-S1-P3	99.7(2)
S2-P2-P3	103.9(1)	P1-S2-P2	103.3(1)
S3-P2-P3	87.47(9)	P2-S3-P2	90.9(2)
P1-Cu1-I1 2×	109.75(6)	P2-Cu2-I2	102.26(9)
P1-Cu1-I1	104.2(1)	P2-Cu2-I2	109.66(6)
I1-Cu1-I1 2×	107.74(5)	P2-Cu2-I2	112.11(6)
I1-Cu1-I1	116.87(6)	I2-Cu2-I2	106.61(4)
		I2-Cu2-I2	106.72(4)
		I2-Cu2-I2	118.08(5)

  0947-6539/02/0818-4229 $ 20.00+.50/0

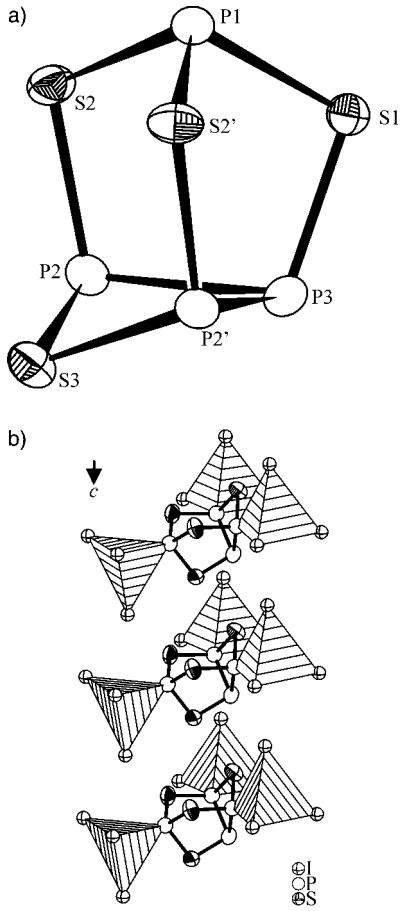

Figure 1. a) Molecular structure and labeling scheme of the C_s-symmetric β-P_4S_4 cage molecules formed in $(CuI)_3P_4S_4$ drawn at the 90% probability level. b) Arrangement of these molecules to a stack running parallel to [001] with tetrahedra separating the single cages from each other. The copper atoms are located within the tetrahedra formed by one P and three I atoms.

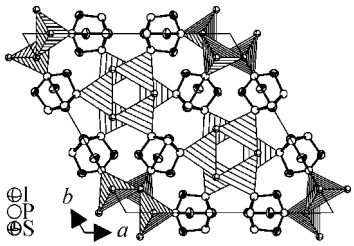

Figure 2. Section of the crystal structure of $(CuI)_3P_4S_4$. β-P_4S_4 cages are coordinated through P1, P2, and P2′ to copper atoms within the tetrahedra. Notice the different orientation of the tetrahedra within different columns.

atom coordinates the cage at the P1 position in $(CuI)_3P_4S_4$. However, since the bond lengths within the cages show no drastic influence due to the different surroundings one can conclude that the interaction between the phosphorus atoms and the metal atoms is only weak. A quite different behavior would be the coordination of a metal atom to the sulfur atoms. To date there are no examples known regardless of the composition of the P–S cage. Very recently the first examples have been reported by using very weakly coordinating anions and Ag^+ as a cation.[11] In these compounds P_4S_3 cages occur that are coordinated to Ag^+ by a sulfur atom.

P and S are hard to distinguish by X-ray diffraction techniques due to their very similar scattering power. Even if the crystal structure of the title compound is isotypic to the homologous selenide it was desirable to confirm the diffraction results by an independent experimental method. Solid-state NMR spectroscpy was chosen because of its proven utility to yield structural information in many ternary metal phosphorus–chalcogenide systems.[3, 12] Figure 3 shows field-dependent ^{65}Cu NMR data of $(CuI)_3P_4S_4$, revealing spectra

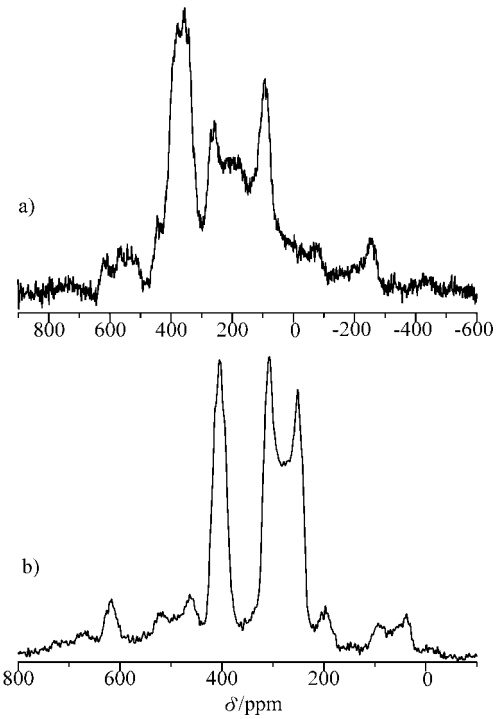

Figure 3. ^{65}Cu MAS NMR spectra of $(CuI)_3P_4S_4$ at a) 7.04 T and b) 11.7 T. Minor peaks are spinning side bands.

characteristic of strong second-order quadrupolar perturbations. Table 4 summarizes the Hamiltonian parameters extracted on the basis of detailed lineshape simulations. Based on the 2:1 intensity ratio the assignment is unambiguous. For both sites the distortion from the tetrahedral symmetry

Table 4. ^{65}Cu NMR-Hamiltonian parameters of $(CuI)_3P_4S_4$.

	δ_{iso} [ppm]	C_Q [MHz]	η	%	χ
Cu1	415	2.75	0.55	36	0.26
Cu2	337	6.89	0.17	64	0.38

caused by Cu–P bonding generates a substantial downfield chemical shift relative to CuI and significant electric field gradients at the copper sites. For quadrupolar nuclei in distorted tetrahedral oxide bonding geometry, values of the nuclear electric quadrupolar coupling constant (NQCC) may be correlated with the distortion parameter (shear strain) [Eq. (1)] reflecting the average deviation from ideal tetrahedral angles. Inspection of Table 3 reveals that both copper sites have similar distorted tetrahedral geometries. Nevertheless, the χ value computed from Equation (1) is signifi-

0947-6539/02/0818-4230 $ 20.00+.50/0 *Chem. Eur. J.* **2002**, *8*, No. 18

cantly smaller for Cu1 than that for Cu2, in good agreement with the difference in nuclear electric quadrupolar coupling constants. This result suggests that semiempirical correlations such as Equation (1) are even applicable for more covalent solids than for oxides, at least at a qualitative level.

$$\chi = \sum_{i=1}^{6} \tan|\alpha_i\text{-}109.48| \quad (1)$$

Figure 4 shows the ^{31}P MAS-NMR spectra at two different magnetic field strengths and spinning frequencies, illustrating the need for very fast spinning in combination with high magnetic field strengths to reach a satisfactory spectral resolution. The three crystallographically distinct phosphorus sites are clearly differentiable in the spectrum recorded at 202.5 MHz. Both the resonance signals of P1 and P2 are split into multiplets owing to dipolar and scalar interactions with the nuclear isotopes ^{63}Cu and ^{65}Cu (both have spin quantum numbers of 3/2) of the directly bonded copper sites Cu1 and Cu2, respectively. This effect is well understood theoretically and arises from the presence of strong nuclear electric quadrupolar interactions experienced by the copper isotopes.[13, 14] These multiplets have been simulated by using the WSOLIDS simulation package created by Eichele and Wasylishen neglecting the small differences in the magnetic dipole moments and the nuclear electric quadrupole moments of the isotopes ^{63}Cu and ^{65}Cu. Table 5 summarizes the simulation parameters used to reproduce the experimental lineshapes. Since the magnitude of the copper quadrupolar coupling constant is known independently from ^{65}Cu NMR spectroscopy and since the value of the ^{31}P–^{63,65}Cu dipole–dipole coupling constant can be computed from the crystal structure, the only adjustable parameters are the isotropic and anisotropic components of the scalar interaction tensors. For J_{iso} a value of 1230 ± 10 Hz yielded the best agreement with the experimental data. In agreement with literature data we further assumed $\Delta J = 500$ Hz, however, our simulations have illustrated that the quality of the fits is not very sensitive to variations in this parameter. The ^{31}P chemical shifts listed in Table 5 for the three phosphorus sites can be compared with solution-state NMR values published for the free-cage molecule β-P_4S_4,[15] where P1, P2, and P3 resonate at 174.7, 207.5, and 85.7 ppm, respectively. This comparison reveals that the coordination with Cu^I leads to pronounced upfield shift effects for P1 and P2, whereas the chemical shift of the non-Cu-bonded P3 site remains nearly unperturbed. Although the peak assignment in Figure 4 is unambiguous, based on the dipolar multiplet structure in combination with the 1:2:1 site multiplicity, further confirmation is desirable. To this end, we can exploit the potential of high-resolution recoupling techniques to correlate the resonance signals of those ^{31}P spins that experience significant ^{31}P–^{31}P direct dipolar or indirect (scalar) interactions.[16, 17] Total-through-bond correlation spectroscopy (TOBSY), which utilizes scalar interactions for achieving polarization transfer, is particularly well-suited for this purpose.[18] Using this technique it is possible to detect selectively correlations between those nuclei that are directly bonded. Recently, Levitt and co-workers have proposed a class of pulse sequences RN_n^ν for efficient dipolar recoupling or decoupling.[19] Thanks to the flexibility and powerful features offered by this class of pulse symmetry, some of the RN_n^ν pulse symmetries are well-suited for TOBSY-like experiments. For example, recent work in our laboratory has shown that the construction of a TOBSY-like experiment based on the $R30_6^{14}$ symmetry (R-TOBSY) is a powerful strategy for *J*-coupling mediated correlation spectroscopy.[20] Figure 5 shows this pulse sequence as used in the present study. The 2D correlation spectrum is shown in Figure 6, which clearly illustrates the presence of direct P2–P3 and the absence of P1–P2 and P1–P3 bond connectivities. Besides confirming the MAS-NMR peak assignment this result indicates the utility of RTOBSY to select direct bond connectivities in strongly coupled spin clusters. This feature should make it a very powerful tool in the structural analysis of crystals, glasses and other material systems with unknown structures.

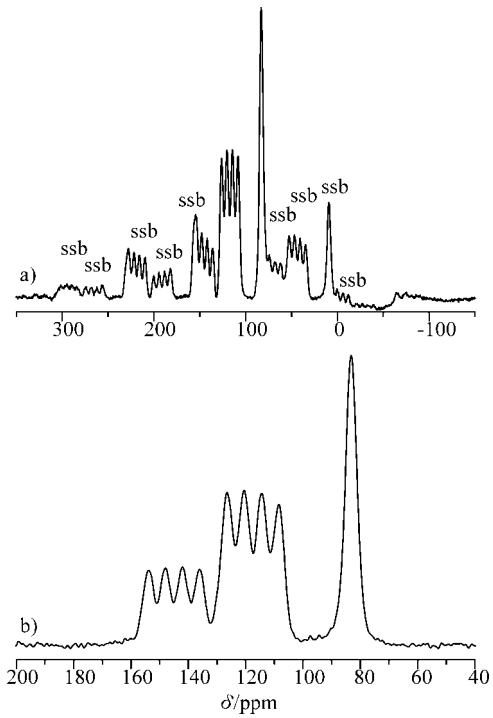

Figure 4. ^{31}P MAS NMR spectra of $(CuI)_3P_4S_4$ at 7.04 T and a spinning frequency of 15 kHz (a) (spinning side bands (ssb) are indicated) and at 11.7 T and a spinning frequency of 30 kHz (b).

Table 5. ^{31}P NMR-Hamiltonian parameters of $(CuI)_3P_4S_4$.

	δ_{iso} [ppm]	D [Hz]	J_{iso} [Hz]	%
P1	144.9	1235	1230	25
P2	117.3	1258	1230	50
P3	83.2	–	–	25

Experimental Section

Syntheses: $(CuI)_3P_4S_4$ was prepared from stoichiometric amounts of CuI, P (ultra high grade, Hoechst), and S (99.999%, Fluka), molar ratio CuI/P/S = 3:4:4. CuI (>98%, Merck) was purified prior to use by recrystallization

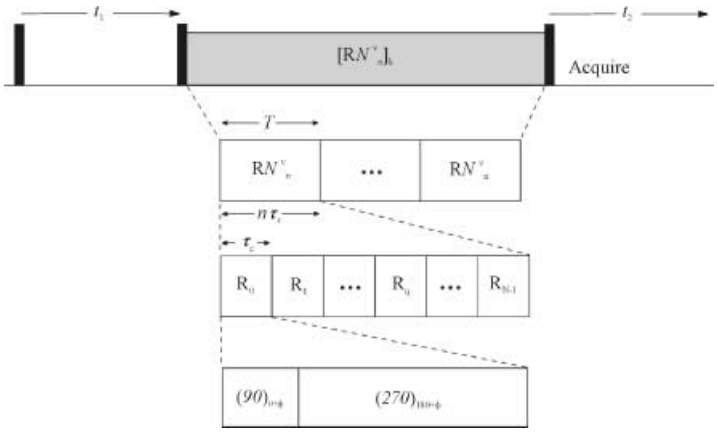

Figure 5. RTOBSY pulse sequence used for the detection of direct $^{31}P-^{31}P$ bond connectivity.[20] Excitation consists of a 90° pulse. The subsequent evolution under the MAS Hamiltonian during t_1 is terminated by a second 90° pulse. The mixing period sandwiched by the second and third 90° pulses comprise k cycles of RN^{ν}_{n} pulse symmetry. T is the complete cycle of the sequence spanning n rotor periods τ_r. τ_c denotes the duration of each subcycle, that is $n\tau_r/N$. The radiofrequency phase of each subcycle R_Q is set equal to $(-1)^q\nu\pi/N$, where q is an index running from 0 to $N-1$, ν is any integer and N must be a positive even integer.

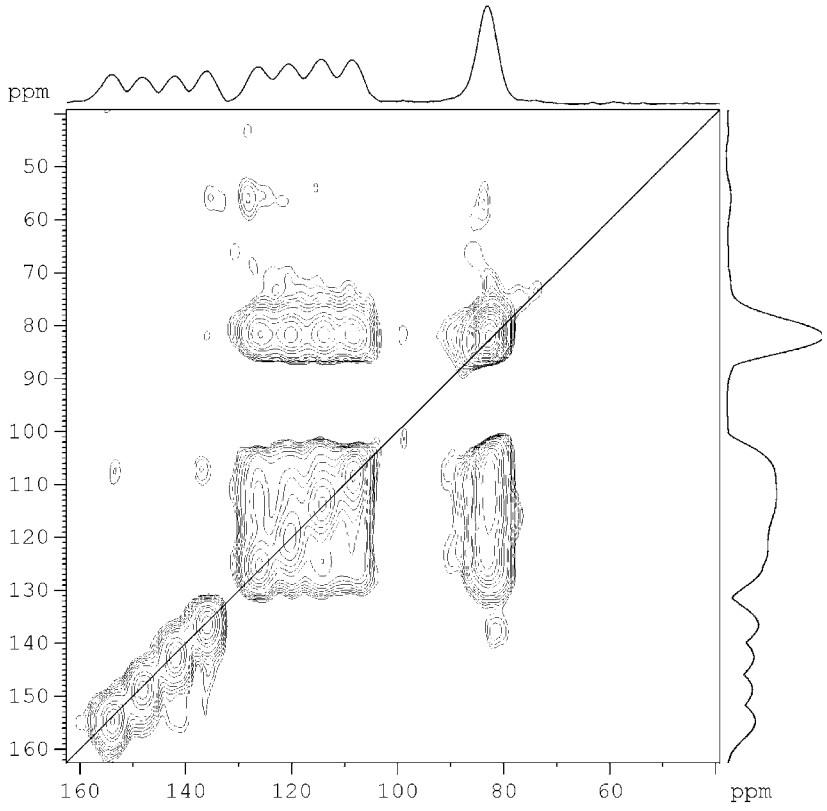

Figure 6. 2D ^{31}P homonuclear correlation spectrum of $(CuI)_3P_4S_4$ obtained by using the RTOBSY sequence of Figure 5 with a mixing time of 4.8 ms.

from concentrated aqueous HI (57%, reinst, Merck). The precipitate was washed several times with demineralized water and ethanol. The resulting white powder was dried in a vacuum for several days.[1] The reaction mixture was slowly heated in evacuated silica ampoules up to 600 °C and then held for three weeks at 270 °C. After homogenization and a second annealing period for two more weeks at 270 °C yellow needle-shaped single crystals suitable for structure determination could be obtained. $(CuI)_3P_4S_4$ forms much slower than $(CuI)_3P_4Se_4$ which can be obtained within a few days. The high viscosity of molten sulfur in this temperature range is supposed as a reason.

Structure determination: Single-crystal X-ray diffraction intensities were collected on a STOE IPDS ($Mo_{K\alpha}$ ($\lambda = 0.71073$ Å)) equipped with a germanium monochromator. Intensity data were corrected for Lorentz and polarization effects, and a numerical absorption correction was performed with an "optimized" shape of the crystal. A total of six crystal faces was used. Minimum and maximum transmission factors were 0.48 and 0.65, respectively. All data handling was done with the STOE program suite.[21] Structure solution and refinement was done with the SHELX97 program package.[10] Inversion twinning was taken into account in the last stage of the refinement. Crystallographic data are summarized in Table 1. The DIAMOND program package was used for visualization purposes.[22] X-ray powder techniques (Siemens D5000, $Cu_{K\alpha 1}$, $\lambda = 1.54051$ Å, Si as an external standard) were employed for purity checks and characterization of powder samples.

NMR spectroscopy: Solid-state ^{65}Cu MAS NMR spectra were obtained at 142.00 MHz using a Bruker DSX-500 NMR spectrometer. Spectra were recorded using small flip angles at an rf nutation frequency of 125 kHz, a relaxation delay of 3s and a MAS rotation frequency of $\nu_r = 30000 \pm 2$ Hz in a 2.5 mm fast-spinning probe. Additional low-field data were recorded at 85.22 MHz on a Bruker CXP-300 spectrometer equipped with a 4 mm MAS-NMR probe (spinning frequency 15 kHz). Lineshape simulation was carried out using the WINFIT[23] simulation package. All chemical shifts are reported relative to solid CuI. All ^{31}P solid-state NMR spectra were obtained on Bruker DSX-400 and 500 NMR spectrometers, equipped with a 2.5 mm fast-spinning probe, operating at a MAS rotation frequency of $\nu_r = 25000 \pm 2$ Hz. For simple 1D spectroscopy, 90° pulses of 2 µs length were used, followed by a relaxation delay of 300 s. Spectra were simulated by using the WINFIT[23] and the WSOLIDS simulation packages. All chemical shifts are reported relative to 85% H_3PO_4.

Solid-state R-TOBSY NMR experiments were carried out at 202.468 MHz, using an rf nutation frequency of $5\nu_r = 125$ kHz. Saturation combs were applied before the relaxation delays for all experiments. The relaxation delay was adjusted to 420 s and eight transients were accumulated for each measurement. The mixing time was varied from 2 ms to 10 ms to adjust optimum conditions.

Acknowledgement

G.B. thanks the Fonds der Chemischen Industrie for a doctoral stipend. J.H.H. gratefully acknowledges a stipend from Oh-Sung Polytechnology Ind. We thank Dr. Klaus Eichele and Dr. Roderick Wasylishen for providing us with access to their WSOLIDS simulation package. This work was financially supported by the Deutsche Forschungsgemeinschaft (DFG) and the Fonds der Chemischen Industrie (FCI).

[1] A. Pfitzner, *Chem. Eur. J.* **2000**, *6*, 1891.
[2] A. Pfitzner, S. Reiser, T. Nilges, *Angew. Chem.* **2000**, *112*, 4328; *Angew. Chem. Int. Ed.* **2000**, *39*, 4160.
[3] A. Pfitzner, S. Reiser, *Inorg. Chem.* **1999**, *38*, 2451.
[4] M. Ruck, *Z. Anorg. Allg. Chem.* **1994**, *620*, 1832.
[5] A. Pfitzner, S. Reiser, H.-J. Deiseroth, *Z. Anorg. Allg. Chem.* **1999**, *625*, 2196.

  0947-6539/02/0818-4232 $ 20.00+.50/0

[6] H. Nowottnick, K. Stumpf, R. Blachnik, H. Reuter, *Z. Anorg. Allg. Chem.* **1999**, *625*, 693.
[7] M. E. Jason, T. Ngo, S. Rahman, *Inorg. Chem.* **1997**, *36*, 2633.
[8] R. Blachnik, A. Hoppe, *Z. Anorg. Allg. Chem.* **1979**, *457*, 91.
[9] A. M. Griffin, P. C. Minshall, G. M. Sheldrick, *J. Chem. Soc. Chem. Commun.* **1976**, *20*, 809.
[10] G. M. Sheldrick, SHELX-97, Program package for crystal structure solution and refinement, Universität Göttingen, Germany, **1997**.
[11] A. Adolf, M. Gonsior, I. Krossing, *J. Am. Chem. Soc.* **2002**, *124*, 7111.
[12] R. H. P. Francisco, H. Eckert, *J. Solid State Chem.* **1994**, *112*, 270.
[13] Menger, W. S. Veeman, *J. Magn. Reson.* **1982**, *46*, 257.
[14] A. C. Olivieri, *J. Am. Chem. Soc.* **1992**, *114*, 5758.
[15] T. Bjorholm, H. Jakobsen, *J. Am. Chem. Soc.* **1991**, *113*, 27.
[16] S. Dusold, J. Kümmerlen, A. Sebald, *J. Phys. Chem. A*, **1992**, *101*, 5895.
[17] J. Schmedt auf der Günne, H. Eckert, *Chem. Eur. J.* **1998**, *4*, 1762.
[18] M. Baldus, B. M. Meier, *J. Magn. Reson. A* **1996**, *121*, 65.
[19] a) M. Carravetta, M. Eden, X. Zhao, A. Brinkmann, M. H. Levitt, *Chem. Phys. Lett.* **2000**, *321*, 205, b) A. Brinkmann, M. H. Levitt, *J. Chem. Phys.* **2001**, *115*, 357.
[20] J. C. C. Chan, G. Brunklaus, *Chem. Phys. Lett.* **2001**, *349*, 104.
[21] STOE, Darmstadt (Germany) **1996**.
[22] K. Brandenburg, DIAMOND Program package for crystal visualization, Version 2.1c, Crystal Impact, Bonn, Germany, **1999**.
[23] D. Massiot, H. Thiele, A. Germanus, *Bruker Report* **1994**, *140*, 43.

Received: April 25, 2002 [F4041]

  0947-6539/02/0818-4233 $ 20.00+.50/0